



DIGITAL ACCESS TO SCHOLARSHIP AT HARVARD

Ecological Boundary Detection Using Bayesian Areal Wombling

The Harvard community has made this article openly available.
[Please share](#) how this access benefits you. Your story matters.

Citation	Fitzpatrick, Matthew C., Evan L. Preisser, Adam Porter, Joseph Elkinton, Lance A. Waller, Bradley P. Carlin, and Aaron M. Ellison. Ecological boundary detection using Bayesian areal wombling. <i>Ecology</i> 91(12): 3448-3455.
Published Version	doi:10.1890/10-0807.1
Accessed	February 19, 2015 7:41:15 AM EST
Citable Link	http://nrs.harvard.edu/urn-3:HUL.InstRepos:4729751
Terms of Use	This article was downloaded from Harvard University's DASH repository, and is made available under the terms and conditions applicable to Open Access Policy Articles, as set forth at http://nrs.harvard.edu/urn-3:HUL.InstRepos:dash.current.terms-of-use#OAP

(Article begins on next page)

1 ECOLOGICAL BOUNDARY DETECTION USING BAYESIAN AREAL WOMBLING

2
3
4 Matthew C. Fitzpatrick^{*1,2,3}, Evan L. Preisser², Adam Porter⁴, Joseph Elkinton⁴, Lance A.
5 Waller⁵, Bradley P. Carlin⁶, Aaron M. Ellison³
6

7 ¹ *University of Maryland Center for Environmental Science, Appalachian Lab, Frostburg, MD*
8 *21532*

9 ² *Department of Biological Sciences, University of Rhode Island, Kingston, RI 02881*

10 ³ *Harvard University, Harvard Forest, Petersham, MA 01366*

11 ⁴ *Department of Plant, Soil, and Insect Sciences, University of Massachusetts at Amherst,*
12 *Amherst, Massachusetts*

13 ⁵ *Department of Biostatistics, Rollins School of Public Health, Emory University*

14 ⁶ *Division of Biostatistics, School of Public Health, University of Minnesota*
15

16 *Author to whom correspondence should be addressed:

17 Matt Fitzpatrick

18 University of Maryland Center for Environmental Science

19 Appalachian Lab

20 301 Braddock Road, Frostburg, MD 21532

21 e-mail: mfitzpatrick@umces.edu; phone: (301) 689-7131; fax: (301) 689-7200
22

23 Manuscript type: *Statistical Report*
24

24 ABSTRACT

25 The study of ecological boundaries and their dynamics is of fundamental importance to much of
26 ecology, biogeography, and evolution. Over the past two decades, boundary analysis (often
27 termed wombling) has received considerable research attention, resulting in multiple approaches
28 for the quantification of ecological boundaries. Nonetheless a number of issues remain
29 unresolved, notably the inability of most methods to (i) analyze spatially-homogenized datasets
30 (i.e., areal data in the form of polygons rather than point-reference data); (ii) account for spatial
31 structure in these data and uncertainty associated with them; and (iii) objectively assign
32 probabilities to boundaries once detected. Here we describe a method for ecological boundary
33 detection used in public health that employs a Bayesian hierarchical framework and which
34 addresses these issues. As examples, we analyze simulated data and the historic pattern of spread
35 of an invasive species, the hemlock woolly adelgid (*Adelges tsugae*), across eastern North
36 America, using county-level dates of first infestation and several covariates potentially important
37 to influencing the observed spread dynamics.

38

39 KEYWORDS: boundary analysis, ecotones, edge detection, invasive species, spatial statistics

40

41 INTRODUCTION

42 A central challenge in ecology is determining the factors influencing species distributions
43 and how these factors change across space and time (Holt and Keitt 2005). The increasingly
44 serious threats to natural systems posed by global change emphasize the practical importance of
45 identifying the environmental factors associated with range edges (e.g., Gavin and Hu 2006) and
46 of determining how environmental changes may affect movement of both native and invasive

47 species across heterogeneous landscapes. At its core, understanding the dynamics of species
48 distributions is both a statistical problem of identifying boundaries between where a species is
49 present (or abundant) and absent (or rare), and an ecological problem of determining
50 environmental factors associated with these boundaries (Gaston 2003, Fortin et al. 2005).

51 Two major challenges limit detailed analysis of ecological and evolutionary processes
52 underlying the formation, persistence, and change of range edges. First, the spatiotemporal data
53 required for inference are lacking (Parmesan et al. 2005) or when available, are often spatially
54 homogenized as summaries over geopolitical or ecological regions such as counties, states, or
55 biomes. Such aggregation obscures fine-scale spatiotemporal characteristics in the data. Second,
56 data arising from neighboring regions are often more highly correlated than those from distant
57 neighbors. The spatial structure inherent in the data is often of ecological interest, but must be
58 accounted for to make valid inferences (Legendre 1993). Acknowledging spatial structure is
59 particularly important when considering the spread of invasive species because ecological
60 dynamics are inherently correlated in space and time.

61 Over the last decade a large body of ecological research has addressed boundary analysis
62 (sometimes called ‘wombling’ in recognition of William H. Womble, a pioneer in the field,
63 Womble 1951), with a corresponding increase in the number of analytical approaches available
64 for detecting and analyzing boundaries (see Jacquez et al. 2000 and Fagan et al. 2003 for recent
65 reviews and Jacquez et al. 2008 for a recent special issue on the topic). Wombling is a technique
66 for determining zones of abrupt change on a spatial surface that separate areas of lower and
67 higher values of a georeferenced unit (Fortin and Dale 2005). A common secondary concern is to
68 assign statistical significance or probabilities to the identified boundaries. At present, much of
69 the published literature on boundary analysis in ecology considers point-referenced data (i.e.,

70 geostatistical data comprised of spatial locations of points with known coordinates, such as
71 latitude-longitude) that are either regularly (lattice or grid) or irregularly spaced. Although point-
72 referenced data are becoming increasingly accessible (Graham et al. 2004), ecological data
73 covering broad spatial and temporal scales are more commonly available as summaries over
74 geographic regions. For example, herbaria data and records from the USDA PLANTS database
75 (<http://plants.usda.gov>) are provided as county- or state-level summaries. Boundary analysis of
76 such data, often term *areal* data, is well-developed in public health fields, but it has received
77 minimal attention in ecology. Further, most of the boundary analysis approaches in current use in
78 ecology assign significance or probabilities to detected boundaries using null distributions or
79 arbitrary thresholds; such inferences are relative to predetermined and often subjective choices.

80 Here we describe a promising technique for ecological analysis of areal data developed
81 by public health researchers (e.g., Lu and Carlin 2005, Ma et al. 2006, Wheeler and Waller 2008)
82 that has as yet seen little use by ecologists. The method employs a Bayesian hierarchical
83 framework that (i) uses areal data; (ii) accounts for spatial structure in these data and the spatial
84 and nonspatial uncertainty associated with them; and (iii) provides a natural means of assigning
85 probabilities to boundaries using posterior estimates of the modeled parameters. As an example,
86 we analyze the historic pattern of spread of an invasive species, the hemlock woolly adelgid
87 ('HWA', *Adelges tsugae* Annand). Although this pest threatens hemlock forests (both eastern
88 hemlock, *Tsuga canadensis* (L.) Carr., and Carolina hemlock, *Tsuga caroliniana* Englemann, are
89 susceptible) throughout eastern North America (Orwig et al. 2002) and is of great concern to
90 both researchers and land managers, data on HWA spread exists primarily as county-level data
91 documenting the first reported HWA infestation in that area. Our goal is to strengthen links
92 between observed spread pattern and underlying ecological processes by identifying boundaries

93 across which spread is slower than expected and to determine whether such boundaries are
94 associated with environment features.

95

96 METHODS

97 *Study system* – HWA is a small (1 mm adult) flightless insect native to Asia that was first
98 collected from hemlock in the eastern United States in spring of 1951, in Richmond, VA. New
99 HWA infestations were collected next in Philadelphia, Pennsylvania in 1969, followed by
100 counties southwest of Richmond, VA (Fig. 1a, see Appendix A for a detailed description of these
101 data). The observed pattern of county-level spread following these early events largely mimics a
102 diffusive process although outlying infestations also have appeared in northwestern New York
103 State. As an exploratory tool, ordinary kriging on the county-level spread pattern (Fig. 1b) shows
104 slow initial spread from the three distinct early infestations, followed by spread to the northeast
105 and southwest. Compressed contours along the Appalachian Mountains suggest that
106 environmental or topographic aspects of this feature may be associated with reduction of spread
107 rate to the west. In contrast, spread has been relatively rapid in the southeastern Appalachians,
108 where contours are spaced broadly (Fig. 1b), suggesting topography alone may not influence
109 spread rate. Despite their proximity to the initial infestation, counties south of Richmond, VA
110 remain uninfested presumably because of a lack of hemlock.

111 Although population and dispersal dynamics of HWA remain poorly understood, we
112 expect the pattern of spread to be a function of both environmental and social factors.
113 Environmental factors such as hemlock abundance and winter temperature (Paradis et al. 2008,
114 Trotter and Shields 2009) may alter spread rate by influencing population and dispersal
115 dynamics. Social factors such as human population density may influence the pattern of spread

116 both by altering the environment (e.g., by reducing forest cover or planting hemlocks as
117 landscape trees) and by influencing the detection and reporting of HWA infestations. To account
118 for these processes, we generated a set of covariates for each county that could influence the
119 spread and detection of the advancing HWA front, including mean winter temperature, human
120 population density, and hemlock abundance (See Appendix A for details regarding the
121 calculation of these variables). We did not consider physical barriers to spread such as rivers or
122 mountains (e.g., Wheeler and Waller 2008) in this analysis because passive dispersal of HWA by
123 wind and birds is unlikely to be directly influenced by such features at the county level.

124

125 *Bayesian areal wombling* – We follow recent work by Lu and Carlin (2005) and use a Bayesian
126 hierarchical model to perform areal wombling. Wheeler and Waller (2008) extended Lu and
127 Carlin’s (2005) research on human disease incidence to the spread of rabies using county-level
128 reporting of rabid raccoons. Following Wheeler and Waller (2008), we modeled Y_i , the number
129 of months elapsed between the first reported HWA infestation in 1951 and the first reported
130 HWA infestation in each county i as

$$131 \quad Y_i \sim N\left(\mu_i, \frac{1}{\tau}\right), \quad (1)$$

132 where

$$133 \quad \mu_i = \alpha + \mathbf{x}_i\beta + \phi_i \quad (2)$$

134 is the expected number of months elapsed to first reported HWA infestation in county i , α is an
135 intercept, τ is the precision, \mathbf{x}_i is a vector of the covariates, and ϕ_i is a spatial random effect. The
136 spatial random effect ϕ_i is given an intrinsic conditionally autoregressive (CAR) prior expressed
137 as

138
$$\phi \sim \text{CAR}(\tau_C), (3)$$

139
$$\phi | \phi_{j \neq i} \sim \text{N}\left(\bar{\phi}_i, \frac{1}{(\tau m_i)}\right), (4)$$

140 where m_i is the number of counties neighboring county i and τ_C is the precision. The use of a
 141 CAR prior for the random effects serves two functions. Foremost, invasive spread is a spatial
 142 process, with neighboring counties more similar in date of first infestation than distant counties.
 143 Second, the CAR prior provides a degree of spatial smoothing and thereby may prevent the
 144 erroneous detection of barriers that arise from spurious departures from the overall spatial trend.
 145 For example, uncertainty in detection and therefore reporting of HWA infestations could be
 146 higher in counties where HWA populations remain at low densities (Fitzpatrick et al. 2009)
 147 because of scarcity of hemlock or where winter temperatures cause high mortality (Paradis et al.
 148 2008, Trotter and Shields 2009). In our analysis, we consider counties to be neighbors if they
 149 share a common boundary; more sophisticated choices such as inverse distance weighting
 150 warrant investigation.

151 The above framework provides a smoothed expected value for the number of months to
 152 first HWA infestation in each county. Although spread rate is itself of ecological interest, our
 153 goal is to identify barriers that separate counties with substantially different times to first
 154 infestation and to assign probabilities to these boundaries. A boundary likelihood value (BLV)
 155 for boundary (i, j) can be defined as the absolute difference in months (Lu and Carlin 2005) of
 156 first HWA infestation reported in neighboring counties i and j as,

157
$$\Delta_{ij} = |Y_i - Y_j|. (5)$$

158 Estimates of Δ_{ij} can be obtained using a Markov chain Monte Carlo (MCMC) algorithm to draw
 159 G samples of the modeled response $\mu_i^{(g)}$, $g = 1, \dots, G$ from the posterior distribution $p(\mu_i | \mathbf{y})$ for

160 each county i and each MCMC iteration g to obtain

$$161 \quad \Delta_{ij}^{(g)} = \left| \mu_i^{(g)} - \mu_j^{(g)} \right|. \quad (6)$$

162 Boundary probabilities are then determined by simply counting the number of samples of $\Delta_{ij}^{(g)}$
163 that exceed a threshold c , where c is some number of months. For example, if we wanted to
164 know which county boundaries were associated with preventing spread for five years (i.e.,
165 difference in date of first detected HWA between adjacent counties is five years), c would equal
166 60 months. The boundary probability is then simply the ratio of this count ($\#\Delta_{ij}^{(g)} > c$) to the total
167 number of samples G (2000 in our analyses), or

$$168 \quad \hat{p}_{ij} \equiv \hat{P}(\Delta_{ij} > c \mid \mathbf{y}) = \frac{\#\Delta_{ij}^{(g)} > c}{G}. \quad (7)$$

169 This approach to determining boundary probabilities is known as fuzzy wombling. Alternatively,
170 crisp wombling can be performed if boundaries are assigned a value of 1 when the BLV exceeds
171 some predetermined threshold (e.g., 0.5) or 0 otherwise.

172 Although BLVs based on the expected values μ_i offer one means of investigating
173 boundary probabilities, a potentially more informative approach is to calculate BLVs using the
174 spatial random effects ϕ_i . In essence, the ϕ_i can be interpreted as spatial residuals. High-
175 probability boundaries based on residuals delineate adjacent regions that differ in their
176 unmodeled heterogeneity and thus highlight regions where the covariates do not explain detected
177 boundaries. In contrast, if no significant boundaries exist in a map of residual-based boundaries,
178 then the covariates explain (or are at least correlated with factors that explain) detected
179 boundaries. Close examination of boundary probabilities based on spatial residuals could prove
180 extremely useful in ecological studies where the goal is to elucidate the factors determining
181 range edges and how these vary across space.

182 The model described above can be fit in WinBUGS (Spiegelhalter et al. 2003) and output
183 analyzed and plotted in R (R Development Core Team 2009). For all models described below we
184 used a burn-in period of 100,000 iterations and an additional 100,000 iterations were used to
185 estimate model parameters. For calculation of BLVs, we subsampled 2000 iterations from the
186 posterior distributions of μ and ϕ . We assessed model convergence using the Gelman-Rubin
187 potential scale reduction statistic (Brooks and Gelman 1998). Details of model construction and
188 selection of priors are available from the code provided in Appendix B.

189

190 EXAMPLE ANALYSES

191 *Simulation study* – Our first example considers an analysis of simulated county-level spread data.
192 We simulated, with added noise, the number of months to first infestation as a linear function of
193 distance from Richmond, VA (Fig. 2a). By design, counties surrounding York County,
194 Pennsylvania do not follow this pattern (Fig. 2b). Because distance from Richmond should not
195 explain the detected boundaries around these outlier counties, even after smoothing, we expect
196 high probability boundaries in the vicinity of York County, PA for both μ - and ϕ -based BLVs.
197 We found the expected pattern: nearly all of the detected boundaries (Fig. 2c) are explained by
198 the covariate other than those surrounding York County, Pennsylvania (Fig. 2d).

199

200 *Historic spread of HWA* – A model fit to the observed HWA spread data incorporated three
201 covariates: human population density, mean winter temperature, and hemlock abundance. This
202 model suggests several features of the spread of HWA (Fig. 3a). Most notably, boundary
203 probabilities are highest (1) in the vicinity of counties where HWA first established and where
204 spread may have been slow due to lag effects (Kowarik 1995) related to HWA population

205 dynamics, (2) along ridges of the Appalachian Mountains north of Tennessee, and (3) in the
206 northernmost portions of HWA's range in New England. In contrast there are few barriers south
207 of Virginia's southern border, where spread has been rapid. However, mean winter temperature
208 and hemlock abundance are not significantly associated with barriers to spread; only the
209 coefficient for human population density emerged as significantly different from zero. Except in
210 for some northern counties and those in central Pennsylvania, boundary probabilities based on
211 the spatial residuals (Fig. 3b) largely reflect those calculated using the expected value μ (Fig.
212 3a).

213 In retrospect, the failure of temperature and hemlock abundance to explain barriers to
214 spread may not be surprising. Global covariates, though useful in detecting and visualizing
215 boundaries, do not couple regional heterogeneity in environmental conditions to local barriers to
216 spread. For example, HWA can spread rapidly under warm temperatures only where hemlock is
217 available. In addition, spread patterns are strongly a function of where propagules are first
218 introduced. In the case of HWA, the earliest dates of infestation are found in counties with little
219 or no naturally-occurring hemlock.

220 To better model the landscape influences that hinder spread, Bayesian spatially-varying
221 coefficient models (Banerjee et al. 2004) can be used for wombling (e.g., Wheeler and Waller
222 2008), although these models offer greater technical challenges. Alternatively, rather than
223 modeling the data arising from areal units, wombling can be performed on the county borders
224 themselves (Ma et al. 2006, Ma et al. 2009). In this approach, every boundary segment is a data
225 point and the response for each segment is the difference in the modeled value of interest
226 between adjacent units. In the context of invasive spread, 'local edge wombling' is likely to be
227 ecologically more sensible because differences (or similarities) between adjacent areal units may

228 be more important for, and therefore may better explain, spread dynamics than mean values of
229 covariates within counties. This approach also provides a more straightforward means to
230 represent physical barriers such as rivers, mountains or urban areas as binary indicator variables.

231 We modified our model (equations 1-3) for local edge wombling by examining the
232 difference in months to first infestation between adjacent counties:

$$233 \quad D_{ij} = Y_i - Y_j, \quad (8)$$

$$234 \quad D_{ij} \sim N\left(\delta_{ij}, \frac{1}{\tau}\right), \quad i \text{ adjacent to } j, \quad (9)$$

235 where

$$236 \quad \delta_{ij} = \alpha + \mathbf{x}_{ij}\beta + \psi_{ij}. \quad (10)$$

237 As before, a spatial random effect (ψ) is included and is given a CAR prior. The vector of
238 covariates \mathbf{x}_{ij} in this version represents *differences* in covariates across borders and/or indicators
239 variables corresponding to known barriers. Because the response is the difference in months to
240 first infestation across borders, the calculation of BLVs is simplified slightly because they are
241 determined using the absolute values of the posterior estimates of δ_{ij} (or ψ_{ij}) themselves (as
242 opposed to *post hoc* calculation of these differences, Eq. 6) using a constant c . Code for fitting
243 this model is provided in Appendix B.

244 A local edge wombling model incorporating as covariates differences in population
245 density, mean winter temperature, and hemlock abundance across county borders reveals similar
246 results to those derived from the areal wombling model: high probability boundaries are
247 concentrated in the east and northeast (Fig. 4a, c). However, the covariates in the local edge
248 wombling model have more influence on the detected boundaries for BLV thresholds of both
249 three (Fig. 4b) and five years (Fig. 4d). The coefficients for hemlock abundance and population

250 density are significantly from zero. As before, boundaries associated with early spread in the
251 eastern portion of the study region remain after accounting for the effects of the covariates,
252 potentially reflecting demographic lag effects unrelated to environmental factors (Kowarik
253 1995).

254

255 CONCLUSIONS

256 Bayesian areal wombling is promising approach for analyzing ecological boundaries and the
257 spread of invasive species. Many other applications for areal wombling can be envisioned. For
258 example, wombling is commonly used in public health research to identify boundaries where
259 disease incidence is higher/lower than expected. The same principle can be applied in ecology to
260 understand patterns of both invasive species richness and distribution as well as patterns of
261 distribution and abundance of native species. Important targets for future improvement of these
262 models in ecology include exploration of alternate parameterizations for spatial smoothing, such
263 as distance weighting or to estimate smoothing parameters from the data (Ma et al. 2009).

264 The strengths of wombling in a Bayesian framework should be clear. Beyond making
265 good use of data with relatively coarse spatial and temporal resolution – data commonly
266 available to ecologists – the Bayesian model easily incorporates uncertainty and provides a
267 natural means of assigning probabilities to detected boundaries. Although there is not yet a single
268 software package or R library that can be used to perform Bayesian areal wombling analyses of
269 the sort described here, the code provided in Appendix B illustrates how to integrate several
270 software packages to implement areal wombling models. Additional statistical challenges
271 remain. The use of a CAR prior encourages local smoothing of dates of first infestation toward
272 those of neighboring counties. Ideally, this accounts for uncertainty in detection, if, for example,

273 a single county reports a much later date of first infestation than its neighbors. Local smoothing
274 can, however, have unanticipated effects. For example, a county that is colonized early but that is
275 surrounded by counties with much later dates of colonization could have a modeled (smoothed)
276 later date of first infestation. Although it is possible for the actual date of first infestation to be
277 earlier than the reported date, it is unlikely that the actual date of first infestation would be later
278 than the reported date (barring misidentification or data entry errors). Finally, the incorporation
279 of spatially-correlated errors may alter estimates of fixed-effects coefficients in ways that are
280 only beginning to be explored and which could lead to misinterpretation of residual-based
281 wombling maps. Despite these issues, Bayesian areal wombling should be considered a
282 complement to existing methods for ecological boundary analysis as one of the few techniques
283 that can effectively utilize the coarse resolution datasets common in ecology and biogeography.

284

285 ACKNOWLEDGEMENTS -

286 We thank D. Wheeler and M. Levine for assistance with coding and for statistical advice. Charlie
287 Burnham, Barbara Burns, Jason Denham, James Johnson, Tom McAvoy, Gary Miller, Dave
288 Orwig, Bradley Register, and Ann Steketee for access to HWA spread datasets. This research
289 was funded by NSF DEB-0715504 to EP and by funding from UMCES to MCF.

290

291 LITERATURE CITED

292 Banerjee, S., B. P. Carlin, and A. E. Gelfand. 2004. Hierarchical Modeling and Analysis for
293 Spatial Data. Chapman & Hall/CRC, Boca Raton, FL.
294 Brooks, S. P., and A. Gelman. 1998. General Methods for Monitoring Convergence of Iterative
295 Simulations. *Journal of Computational and Graphical Statistics* 7:434-455.

296 Fagan, W. F., M. J. Fortin, and C. Soykan. 2003. Integrating edge detection and dynamic
297 modeling in quantitative analyses of ecological boundaries. *BioScience* 53:730-738.

298 Fitzpatrick, M. C., E. L. Preisser, A. M. Ellison, and J. S. Elkinton. 2009. Observer bias and the
299 detection of low-density populations. *Ecological Applications* 19:1673-1679.

300 Fortin, M. J., T. H. Keitt, B. A. Maurer, M. L. Taper, D. M. Kaufman, and T. M. Blackburn.
301 2005. Species' geographic ranges and distributional limits: pattern analysis and statistical
302 issues. *Oikos* 108:7-17.

303 Fortin, M., and M. R. T. Dale. 2005. *Spatial Analysis*. Cambridge University Press, Cambridge.

304 Gaston, KJ 2003. *The structure and dynamics of geographic ranges*. Oxford Univ. Press, Oxford.

305 Gavin, DG and FS Hu. 2006. Spatial variation of climatic and non-climatic controls on species
306 distribution: the range limit of *Tsuga heterophylla*. *Journal of Biogeography* 33:1384-1396.

307 Graham, C. H., S. Ferrier, F. Huettman, C. Moritz, and A. T. Peterson. 2004. New developments
308 in museum-based informatics and applications in biodiversity analysis. *Trends in Ecology &*
309 *Evolution* 19:497-503.

310 Holt, R. D., and T. H. Keitt. 2005. Species' borders: a unifying theme in ecology. *Oikos* 108:3-6.

311 Jacquez, G., M. Fortin, and P. Goovaerts. 2008. Preface to the special issue on spatial statistics
312 for boundary and patch analysis. *Environmental and Ecological Statistics* 15:365-367.

313 Jacquez, G. M., S. Maruca, and M. Fortin. 2000. From fields to objects: A review of geographic
314 boundary analysis. *Journal of Geographical Systems* 2:221-241.

315 Kowarik, I. 1995. Time lags in biological invasions with regard to the success and failure of
316 alien species. *in* P. Pysek, K. Prach, M. Rejmanek, and M. Wade, editors. *Plant Invasions -*
317 *General Aspects and Special Problems*. SPB Academic Publishing, Amsterdam.

318 Legendre, P. 1993. Spatial Autocorrelation - Trouble or New Paradigm. *Ecology* 74:1659-1673.

319 Lu, H., and B. P. Carlin. 2005. Bayesian Areal Wombling for Geographical Boundary Analysis.
320 Geographical Analysis 37:265-285.

321 Ma, H., B. P. Carlin, and S. Banerjee. In Press. Hierarchical and Joint Site-Edge Methods for
322 Medicare Hospice Service Region Boundary Analysis. Biometrics.

323 Ma, H., B. A. Virnig, and B. P. Carlin. 2006. Spatial methods in areal administrative data
324 analysis. Italian Journal of Public Health 3:94-103.

325 Orwig, DA, D Foster, DL Mauseel. 2002. Landscape patterns of hemlock decline in New England
326 due to the introduced hemlock woolly adelgid. Journal of Biogeography 29:1475-1487.

327 Paradis, A., J. Elkinton, K. Hayhoe, and J. Buonaccorsi. 2008. Role of winter temperature and
328 climate change on the survival and future range expansion of the hemlock woolly adelgid
329 (*Adelges tsugae*) in eastern North America. Mitigation and Adaptation Strategies for Global
330 Change 13:541-554.

331 Parmesan, C., S. Gaines, L. Gonzalez, D. M. Kaufman, J. Kingsolver, A. Townsend Peterson,
332 and R. Sagarin. 2005. Empirical perspectives on species borders: from traditional
333 biogeography to global change. Oikos 108:58-75.

334 R Development Core Team. 2009. R: A language and environment for statistical computing. R
335 Foundation for Statistical Computing, Vienna, Austria.

336 Spiegelhalter, D., A. Thomas, N. Best, and D. Lunn. 2003. WinBUGS Users Manual, v 1.4.3.

337 Trotter, R. T., and K. S. Shields. 2009. Variation in Winter Survival of the Invasive Hemlock
338 Woolly Adelgid (Hemiptera: Adelgidae) Across the Eastern United States. Environmental
339 Entomology 38:577-587.

340 Wheeler, D., and L. Waller. 2008. Mountains, valleys, and rivers: The transmission of raccoon
341 rabies over a heterogeneous landscape. Journal of Agricultural, Biological, and Environmental

342 Statistics 13:388-406.

343 Womble, W. H. 1951. Differential Systematics. Science 114:315-322.

344

345 FIGURE LEGENDS

346 Figure 1. Observed pattern of spread of the hemlock woolly adelgid at (a) the county level and
347 (b) smoothed using ordinary kriging of these dates. Colors represent the number of months
348 elapsed since the first reported infestation in Richmond, VA (red star) in 1951 and the first
349 reported infestation in each county.

350

351 Figure 2. Bayesian areal wombling on (a) simulated dates of first infestation; and (b) a single
352 simulated covariate related to distance from Richmond, VA, with a cluster of outlier counties
353 centered on York County, PA (red shading). Panels (c) and (d) show posterior probabilities for
354 boundaries for the expected values μ and the spatial residuals ϕ respectively and a threshold of
355 60 months. Darker shades of red indicate high boundary probabilities.

356

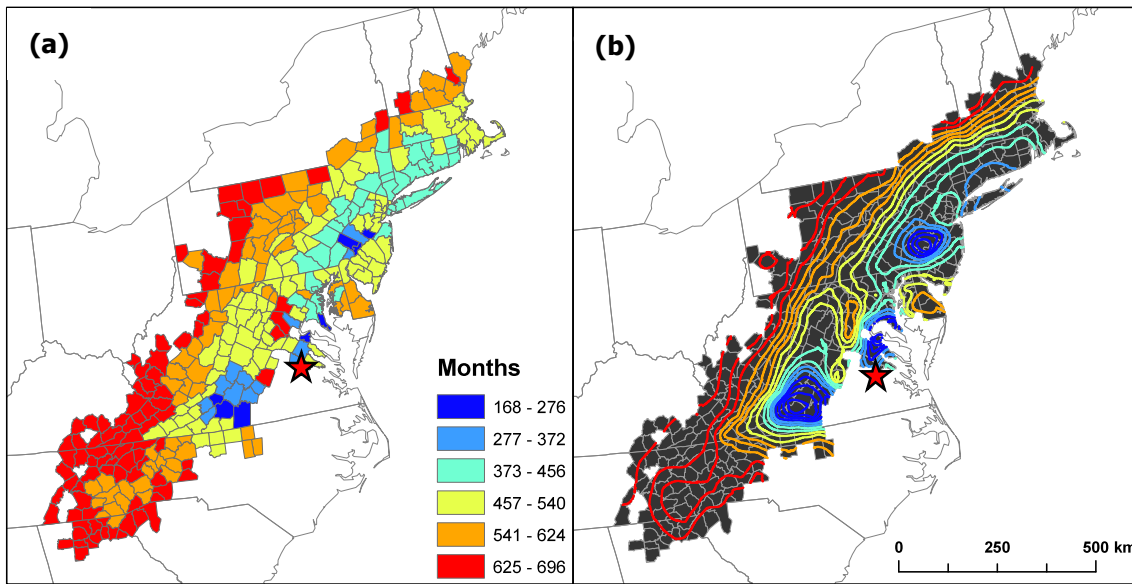
357 Figure 3. Posterior probabilities for Bayesian areal wombling boundaries calculated using either
358 (a) the expected values μ or (b) the spatial residuals ϕ and a threshold of 60 months. Darker
359 shades of red indicate high boundary probabilities.

360

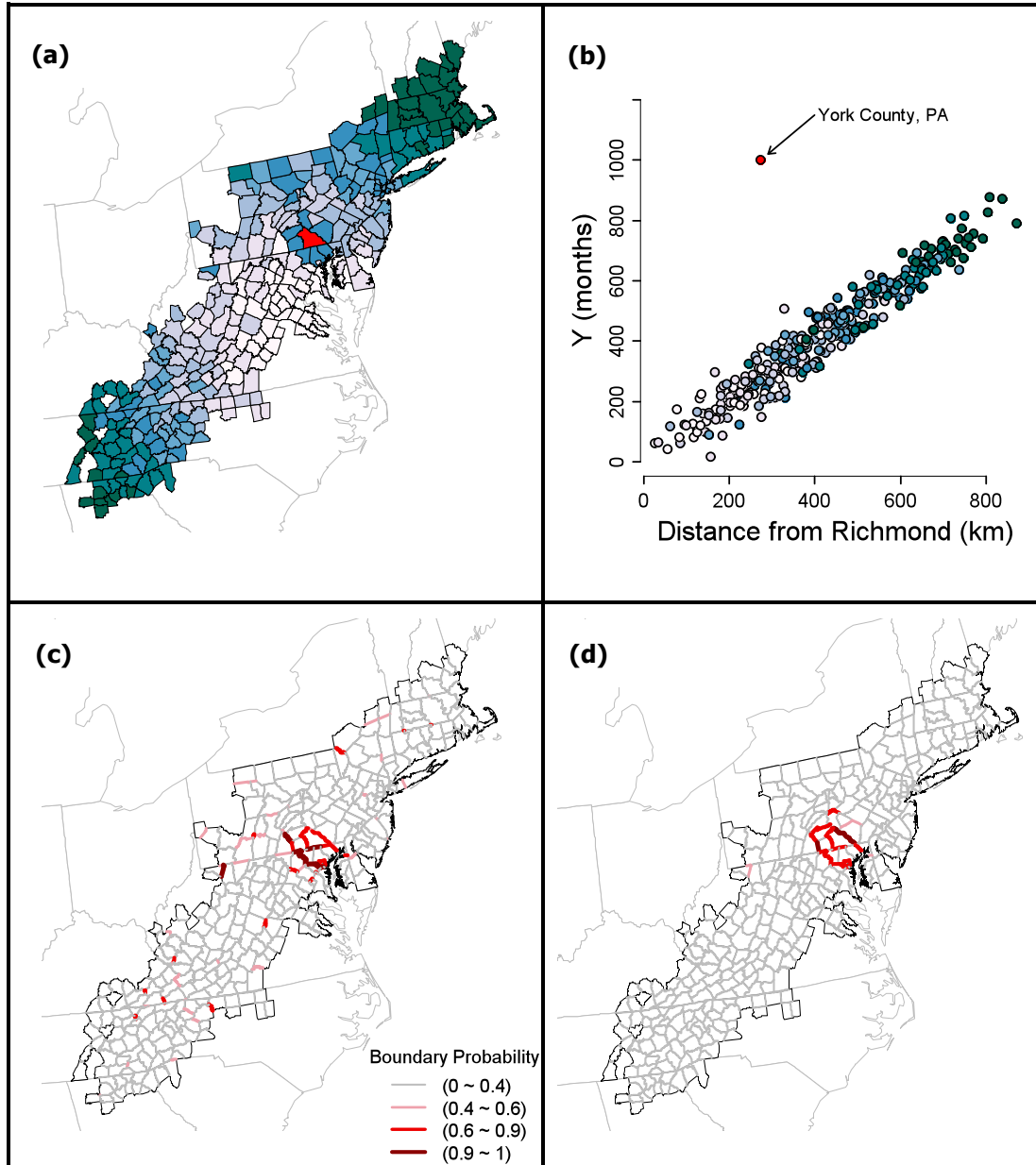
361 Figure 4. Posterior probabilities for Bayesian local edge wombling boundaries calculated using
362 either (a) the expected values δ or (b) the spatial residuals ψ and a threshold of 36 months.

363 Panels (c) and (d) show the same, but using a threshold of 60 months. Darker shades of red
364 indicate high boundary probabilities.

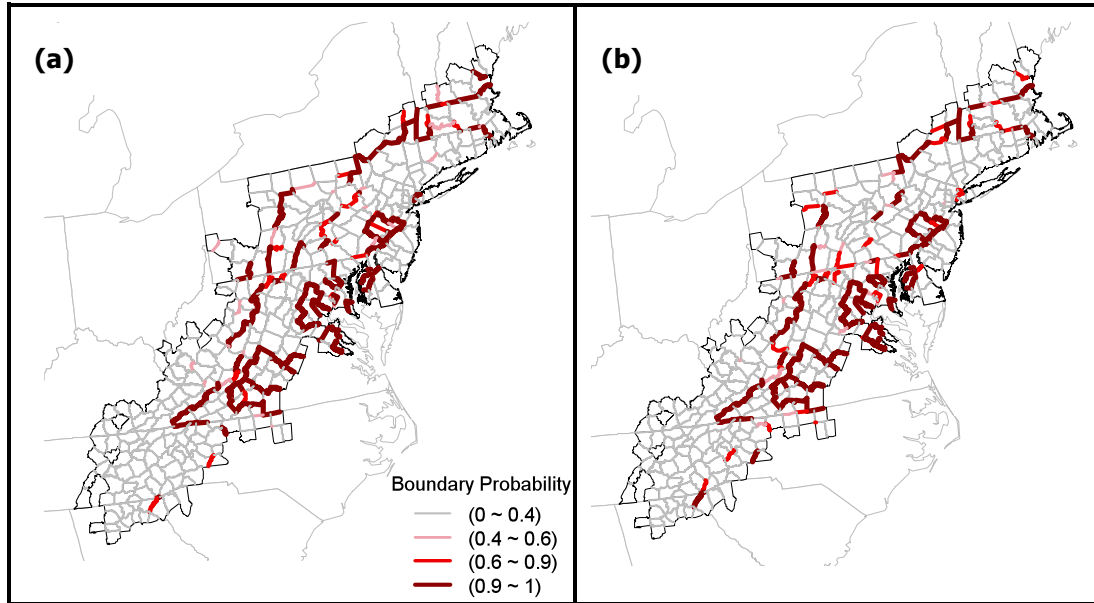
365 Figure 1.



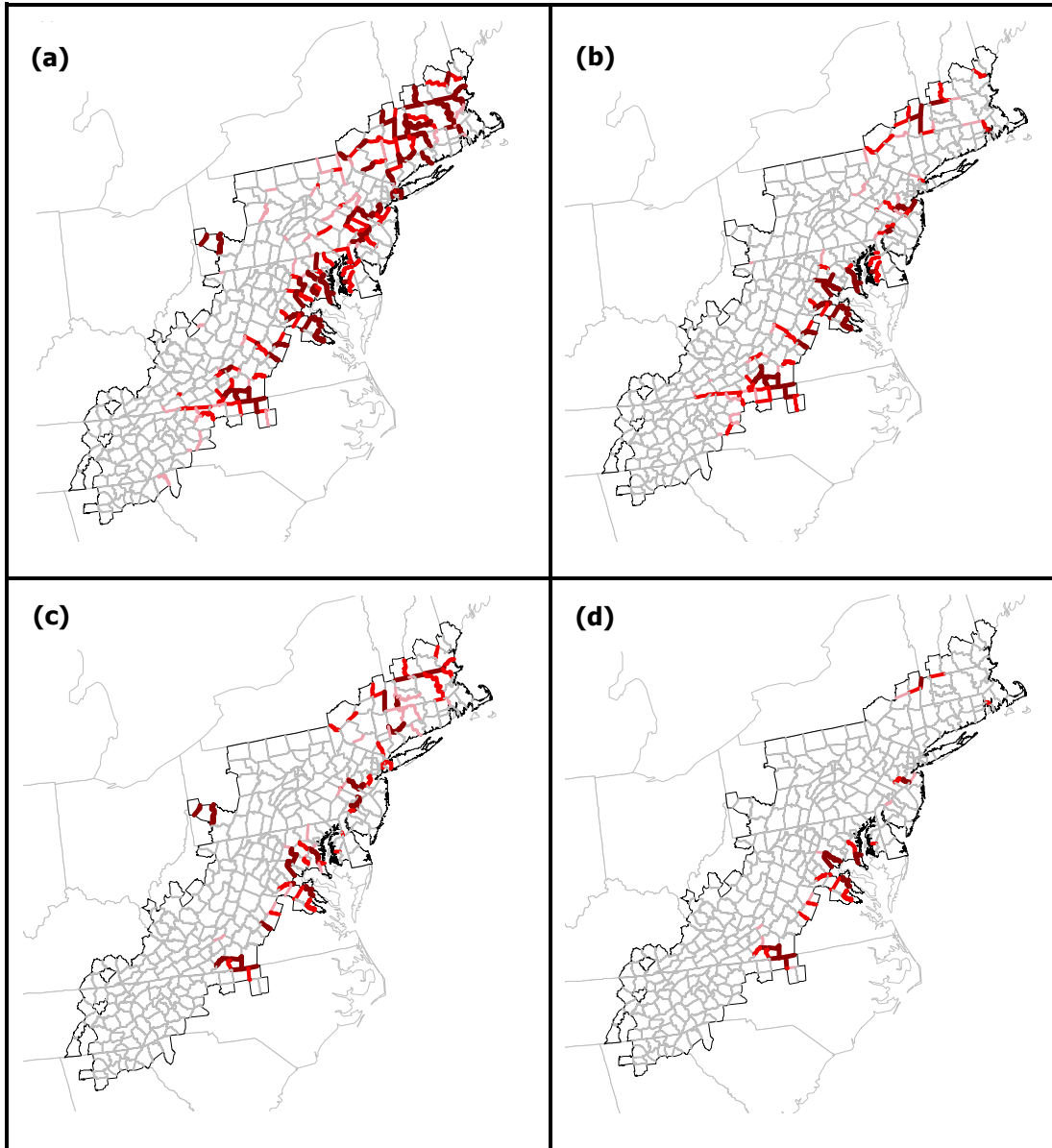
366



368 Figure 3.



369



1 APPENDIX A – Description of datasets

2

3 *County-level spread records* - We derived the dynamics of HWA’s spread for the years 1951
4 through 2009 using county-level records compiled by Forest Service, US Department of
5 Agriculture, Forest Health Protection personnel
6 (<http://na.fs.fed.us/fhp/hwa/maps/distribution.shtm>). We updated these county-level records with
7 more localized records drawn from multiple sources, including: the National Entomological
8 Collection at the Smithsonian Institute (G. Miller), the Pennsylvania General Hemlock Survey
9 executed by the Pennsylvania Department of Conservation of Natural Resources (B. Regester),
10 township-level records for Massachusetts (C. Burnham) and New York (J. Denham), surveys
11 performed by the Georgia Forestry Commission (J. Johnson), stand-level surveys for
12 southwestern Virginia (T. McAvoy), surveys in southern Vermont by the Vermont Department
13 of Forests, Parks, & Recreation (B. Burns), and stand-level surveys in Connecticut and
14 Massachusetts (D. Orwig). When these more local surveys indicated an earlier date of first
15 infestation than the county-level records, we updated the county-level records as necessary.
16 Finally, to simplify coding of the models, we removed 12 “island” counties, (i.e., counties with
17 no infested neighbors possibly infested by long-distance jump dispersal). The final dataset
18 comprised 322 counties with dates of first infestation ranging from 1951 to 2009.

19

20 *Estimates of hemlock abundance* - To produce a map of hemlock abundance we used the
21 randomForests algorithm (Liaw and Wiener 2002) in R 2.9.1 (R Development Core Team 2009)
22 to relate observed hemlock abundance (basal area, $m^2 ha^{-1}$) from the USDA Forest Inventory and
23 Analysis (FIA) database (comprised of 16,084 occurrences) to 26 environmental predictor

24 variables. Environment predictors included 23 bioclimatic variables describing minimum,
25 maximum, and seasonality in temperature and precipitation and water balance (Hijmans et al.
26 2005, Svenning and Skov 2005), two topographic variables (slope and compound topography
27 index) from the USGS HYDRO1k dataset
28 (http://eros.usgs.gov/#/Find_Data/Products_and_Data_Available/gtopo30/hydro), and an index
29 of net primary productivity (Zhao et al. 2005). All variables were manipulated in ArcGIS 9.3
30 such that they were spatially congruent, had a common resolution of 1 km, and were projected
31 using an equidistance conic projection to preserve distance characteristics between locations.

32 We used the resulting model to predict hemlock abundance across eastern North
33 America. Although Carolina hemlock (*Tsuga caroliniana*) is also susceptible to HWA, we did
34 not model its distribution as it is relatively rare and narrowly distributed and its distribution falls
35 entirely within the range of eastern hemlock. To account for the fact that most cells were not
36 100% forested, we multiplied the map of hemlock abundance by a corresponding remotely-
37 sensed estimate of percent forest cover. The result was a map of hemlock abundance adjusted for
38 forest cover that corresponds well with its known distribution and abundance.

39
40 *Estimate of human population density & mean winter temperature* – Estimates of human
41 population density were derived from 2000 U.S. census data
42 (<http://www.census.gov/main/www/cen2000.html>). Estimates of mean winter temperature
43 (December, January, February, March) at 1km spatial resolution were downloaded from the
44 Worldclim database (<http://www.worldclim.org/>, Hijmans et al. 2005). For all covariates, we
45 used the Zonal Statistics tool in ArcGIS 9.3 to calculate summaries of covariates for each
46 county.

47 LITERATURE CITED

- 48 Hijmans, R. J., S. E. Cameron, J. L. Parra, P. G. Jones, and A. Jarvis. 2005. Very high resolution
49 interpolated climate surfaces for global land areas. *International Journal of Climatology*
50 25:1965-1978. doi: 10.1002/joc.1276.
- 51 Liaw, A., M. Wiener 2002. Classification and regression by Random Forest. *R News*. 2: 18-22.
- 52 R Development Core Team. 2009. R: A language and environment for statistical computing. R
53 Foundation for Statistical Computing, Vienna, Austria. Retrieved from [http://www.R-](http://www.R-project.org)
54 [project.org](http://www.R-project.org).
- 55 Svenning, J. C., and F. Skov. 2005. The relative roles of environment and history as controls of
56 tree species composition and richness in Europe. *Journal of Biogeography* 32:1019-1033.
- 57 Zhao, M., F. A. Heinsch, R. R. Nemani, and S. W. Running. (2005). Improvements of the
58 MODIS terrestrial gross and net primary production global data set. *Remote Sensing of*
59 *Environment*. 95: 164.176.

60 APPENDIX B – WinBUGS Code

61

```

# MODEL: three global covariates, spatial error

# WinBUGS model to perform Bayesian areal wombling (boundary detection) with
# global covariates

# Y is time to first infestation: the number of months elapsed, for each county
# i, since the first report of hemlock woolly adelgid in eastern North America
# in 1951 (e.g., if a county was found to be infested in 1981, Y = 360)

# code is called from R using R2WinBUGS

model{
  # Likelihood
  for (i in 1:n.areas){
    Y[i] ~ dnorm(mu[i], tau.err)

    mu[i] <- beta[1] + beta[2]*X1[i] + beta[3]*X2[i] + beta[4]*X3[i] + phi[i]

    # vector for plotting
    SLDRhat[i] <- mu[i] # SLDR, standardized late detection ratio,
                       # is legacy terminology from B. Carlin's code and
                       # has no meaning in this context
  }

  # CAR prior for the spatial random effects
  phi[1:n.areas] ~ car.normal(adj[], weights[], num[], tau.phi) # CAR prior
  for (k in 1:sumNumNeigh){weights[k] <- 1}

  # Other priors
  beta[1] ~ dflat()
  beta[2] ~ dnorm(0, 0.000001)
  beta[3] ~ dnorm(0, 0.000001)
  beta[4] ~ dnorm(0, 0.000001)

  tau.phi <- 1/pow(sdphi, 2)
  tau.err <- 1/pow(sdy, 2)
  sdphi ~ dunif(0,150)
  sdy ~ dunif(0,100)
}

```

62 }

```

# WinBUGS model to perform Bayesian local edge wombling (boundary detection)
# with three covariates & spatial error

# Y is the DIFFERENCE in time to first infestation

# Covariates are differences in values across edges

# Must have separate chunks of code for each edge without neighbors,
# 15 in this example

# code is called from R using R2WinBUGS

model{
  # Likelihood

  Y[1] ~ dnorm(mu[1], tau.err)
  mu[1] <- beta[1] + beta[2]*X1[1] + beta[3]*X2[1] + beta[4]*X3[1] + psi[1] + phi[1]
  #psi term is to account for island edges that have no neighbors

  # vector for plotting
  SLDRhat[1] <- mu[1] # SLDR, standardized late detection ratio,
                     # is legacy terminology from B. Carlin code and has no
                     # meaning in this context

  for (i in 2:38){
    Y[i] ~ dnorm(mu[i], tau.err)
    mu[i] <- beta[1] + beta[2]*X1[i] + beta[3]*X2[i] + beta[4]*X3[i] + phi[i]
    SLDRhat[i] <- mu[i]}

  Y[39] ~ dnorm(mu[39], tau.err)
  mu[39] <- beta[1] + beta[2]*X1[39] + beta[3]*X2[39] + beta[4]*X3[39] + psi[2] + phi[39]
  SLDRhat[39] <- mu[39]

  for (i in 40:46){
    Y[i] ~ dnorm(mu[i], tau.err)
    mu[i] <- beta[1] + beta[2]*X1[i] + beta[3]*X2[i] + beta[4]*X3[i] + phi[i]
    SLDRhat[i] <- mu[i]}

  Y[47] ~ dnorm(mu[47], tau.err)
  mu[47] <- beta[1] + beta[2]*X1[47] + beta[3]*X2[47] + beta[4]*X3[47] + psi[3] + phi[47]
  SLDRhat[47] <- mu[47]

  for (i in 48:110){
    Y[i] ~ dnorm(mu[i], tau.err)
    mu[i] <- beta[1] + beta[2]*X1[i] + beta[3]*X2[i] + beta[4]*X3[i] + phi[i]
    SLDRhat[i] <- mu[i]}

  Y[111] ~ dnorm(mu[111], tau.err)
  mu[111] <- beta[1] + beta[2]*X1[111] + beta[3]*X2[111] + beta[4]*X3[111] + psi[4] + phi[111]
  SLDRhat[111] <- mu[111]

  for (i in 112:155){
    Y[i] ~ dnorm(mu[i], tau.err)
    mu[i] <- beta[1] + beta[2]*X1[i] + beta[3]*X2[i] + beta[4]*X3[i] + phi[i]
    SLDRhat[i] <- mu[i]}

  Y[156] ~ dnorm(mu[156], tau.err)
  mu[156] <- beta[1] + beta[2]*X1[156] + beta[3]*X2[156] + beta[4]*X3[156] + psi[5] + phi[156]

```

```

SLDRhat[156] <- mu[156]

for (i in 157:276){
  Y[i] ~ dnorm(mu[i], tau.err)
  mu[i] <- beta[1] + beta[2]*X1[i] + beta[3]*X2[i] + beta[4]*X3[i] + phi[i]
  SLDRhat[i] <- mu[i]}

Y[277] ~ dnorm(mu[277], tau.err)
mu[277] <- beta[1] + beta[2]*X1[277] + beta[3]*X2[277] + beta[4]*X3[277] + psi[6] + phi[277]
SLDRhat[277] <- mu[277]

for (i in 278:282){
  Y[i] ~ dnorm(mu[i], tau.err)
  mu[i] <- beta[1] + beta[2]*X1[i] + beta[3]*X2[i] + beta[4]*X3[i] + phi[i]
  SLDRhat[i] <- mu[i]}

Y[283] ~ dnorm(mu[283], tau.err)
mu[283] <- beta[1] + beta[2]*X1[283] + beta[3]*X2[283] + beta[4]*X3[283] + psi[7] + phi[283]
SLDRhat[283] <- mu[283]

for (i in 284:370){
  Y[i] ~ dnorm(mu[i], tau.err)
  mu[i] <- beta[1] + beta[2]*X1[i] + beta[3]*X2[i] + beta[4]*X3[i] + phi[i]
  SLDRhat[i] <- mu[i]}

Y[371] ~ dnorm(mu[371], tau.err)
mu[371] <- beta[1] + beta[2]*X1[371] + beta[3]*X2[371] + beta[4]*X3[371] + psi[8] + phi[371]
SLDRhat[371] <- mu[371]

for (i in 372:445){
  Y[i] ~ dnorm(mu[i], tau.err)
  mu[i] <- beta[1] + beta[2]*X1[i] + beta[3]*X2[i] + beta[4]*X3[i] + phi[i]
  SLDRhat[i] <- mu[i]}

Y[446] ~ dnorm(mu[446], tau.err)
mu[446] <- beta[1] + beta[2]*X1[446] + beta[3]*X2[446] + beta[4]*X3[446] + psi[9] + phi[446]
SLDRhat[446] <- mu[446]

for (i in 447:473){
  Y[i] ~ dnorm(mu[i], tau.err)
  mu[i] <- beta[1] + beta[2]*X1[i] + beta[3]*X2[i] + beta[4]*X3[i] + phi[i]
  SLDRhat[i] <- mu[i]}

Y[474] ~ dnorm(mu[474], tau.err)
mu[474] <- beta[1] + beta[2]*X1[474] + beta[3]*X2[474] + beta[4]*X3[474] + psi[10] + phi[474]
SLDRhat[474] <- mu[474]

for (i in 475:580){
  Y[i] ~ dnorm(mu[i], tau.err)
  mu[i] <- beta[1] + beta[2]*X1[i] + beta[3]*X2[i] + beta[4]*X3[i] + phi[i]
  SLDRhat[i] <- mu[i]}

Y[581] ~ dnorm(mu[581], tau.err)
mu[581] <- beta[1] + beta[2]*X1[581] + beta[3]*X2[581] + beta[4]*X3[581] + psi[11] + phi[581]
SLDRhat[581] <- mu[581]

for (i in 582:673){
  Y[i] ~ dnorm(mu[i], tau.err)
  mu[i] <- beta[1] + beta[2]*X1[i] + beta[3]*X2[i] + beta[4]*X3[i] + phi[i]

```

```

SLDRhat[i] <- mu[i]}

Y[674] ~ dnorm(mu[674], tau.err)
mu[674] <- beta[1] + beta[2]*X1[674] + beta[3]*X2[674] + beta[4]*X3[674] + psi[12] + phi[674]
SLDRhat[674] <- mu[674]

for (i in 675:698){
  Y[i] ~ dnorm(mu[i], tau.err)
  mu[i] <- beta[1] + beta[2]*X1[i] + beta[3]*X2[i] + beta[4]*X3[i] + phi[i]
  SLDRhat[i] <- mu[i]
}

Y[699] ~ dnorm(mu[699], tau.err)
mu[699] <- beta[1] + beta[2]*X1[699] + beta[3]*X2[699] + beta[4]*X3[699] + psi[13] + phi[699]
SLDRhat[699] <- mu[699]

for (i in 700:723){
  Y[i] ~ dnorm(mu[i], tau.err)
  mu[i] <- beta[1] + beta[2]*X1[i] + beta[3]*X2[i] + beta[4]*X3[i] + phi[i]
  SLDRhat[i] <- mu[i]}

Y[724] ~ dnorm(mu[724], tau.err)
mu[724] <- beta[1] + beta[2]*X1[724] + beta[3]*X2[724] + beta[4]*X3[724] + psi[14] + phi[724]
SLDRhat[724] <- mu[724]

for (i in 725:739){
  Y[i] ~ dnorm(mu[i], tau.err)
  mu[i] <- beta[1] + beta[2]*X1[i] + beta[3]*X2[i] + beta[4]*X3[i] + phi[i]
  SLDRhat[i] <- mu[i]}

Y[740] ~ dnorm(mu[740], tau.err)
mu[740] <- beta[1] + beta[2]*X1[740] + beta[3]*X2[740] + beta[4]*X3[740] + psi[15]+ phi[740]
SLDRhat[740] <- mu[740]

for (i in 741:793){
  Y[i] ~ dnorm(mu[i], tau.err)
  mu[i] <- beta[1] + beta[2]*X1[i] + beta[3]*X2[i] + beta[4]*X3[i] + phi[i]
  SLDRhat[i] <- mu[i]}

# CAR prior for the spatial random effects
phi[1:n.areas] ~ car.normal(adj[], weights[], num[], tau) # CAR prior
for (k in 1:sumNumNeigh){weights[k] <- 1}

# prior for edges without neighbors
for (j in 1:15) {psi[j] ~ dnorm(0, tau.psi)}

# Other priors
beta[1] ~ dflat()
beta[2] ~ dnorm(0, 0.000001)
beta[3] ~ dnorm(0, 0.000001)
beta[4] ~ dnorm(0, 0.000001)

tau <- 1/pow(sdphi,2) #per Andrew Lawson
tau.err <- 1/pow(sdy,2)
tau.psi <- 1/pow(sdpsi,2)
sdphi ~ dunif(0, 100)
sdy ~ dunif(0, 100)
sdpsi ~ dunif(0, 100)
}

```

```

1 #####
2 # R code to prepare data, call winBUGS code to perform Bayesian wombling,
3 # and plot output.
4 #
5 # 21 April 2010
6 # M. C. Fitzpatrick
7 # mfitzpatrick@umces.edu
8 #
9 # Most of this code is based on hard work by Brad Carlin & his students/post-
10 # docs. I have simply assembled many pieces into one place.
11 # In some instances, files available from:
12 # http://www.biostat.umn.edu/~brad
/software.html are needed. See comments below.
13 #
14 # The analyses require a shapefile with a response of interest (in this case
15 # month of first infestation) and corresponding covariates
16 #####
17
18
19 ### chunk 1 - set wd and load libraries #####
20 setwd("...")
21 source("womblingFuncs.R")
22 library(R2WinBUGS)
23 library(maptools)
24 library(spdep)
25 library(coda)
26 library(RColorBrewer)
27 library(classInt)
28 library(sp)
29 #####
30
31
32 ### chunk 2 - build adjacency & edge info #####
33 # Given a shapefile, this R code creates:
34 # (1) an areal adjacency matrix using maptools,
35 # (2) an edge adjacency matrix (indicating which edges touch each other)
36
37 # based on code provided from B. Carlin's website:
38 # http://www.biostat.umn.edu/~brad/software/getEdges_code.txt
39
40 # Also will need following two .exe files from B. Carlin's website
41 # (1) matchzip.exe
42 # (2) edgeneig.exe
43 # downloaded from: http://www.biostat.umn.edu/~brad/software/tutorial.zip
44
45 setwd("../edgefolder")
46 # output files will be saved under current directory
47 # copy "matchzip.exe" and "edgeneig.exe" to directory "edgefolder"
48

```

```

49 map <- readShapeSpatial("../hwa_wombling.shp")
50
51 # Use maptools to get polygon adjacency matrix
52 # two areas are neighbors if they share common edges with length > 0
53 nb.r <- poly2nb(map, queen=F)
54 mat <- nb2mat(nb.r, style="B") # mat is the 0/1 adjacency matrix
55 n.site <- dim(mat)[1] # n.site: number of areas
56 n.edge <- sum(mat)/2 # n.edge: number of unique pairs
57
58
59 SEind1 <- SEind2 <- 0
60 matmy <- mat
61 for(i in 1:(n.site-1)){
62   for(j in (i+1):n.site){
63     if (mat[i,j]>0) {SEind1<-c(SEind1,i)
64       SEind2<-c(SEind2,j)
65       matmy[i,j]<-matmy[j,i]<-length(SEind1)-1
66     }
67   }
68 }
69
70 SEind1 <- SEind1[-1] # edges sorted by row of upper triangle of the adj. matrix
71 SEind2 <- SEind2[-1] # SEind1[k]=i and SEind2[k]=j => kth edge is edge ij
72
73 dput(SEind1,"SEind1.txt")
74 dput(SEind2,"SEind2.txt")
75 dput(mat, "W.txt")
76
77 # create adjacency information needed for WinBUGS
78 mkAdj <- function(W){
79   n <- nrow(W)
80   adj <- 0
81   for(i in 1:n){
82     for(j in 1:n){
83       if(W[i,j]==1){adj<-append(adj,j)
84     }
85   }
86 }
87 adj <- adj[-1]
88 return(adj)
89 }
90
91 dput(mkAdj(mat),"Sadj.txt")
92 dput(as.vector(rowSums(mat)),"Snum.txt")
93
94 # Create adj. matrix for the edges
95
96 # 1. prepare needed files and save them #
97 # under the directory where you have #
98 # matchzip.exe and edgeneig.exe #
99

```

```

100 # Dump out the coordinates (by polygon) #
101 # Default order for polygons is by first column of map@data #
102
103 for(i in 1:n.site){
104     write(t(map@polygons[[i]]@Polygons[[1]]@coords), paste(i, ".txt", sep=""),
105           ncolumns=2)
106 }
107
108 # Dump out SEind, the site-edge correspondence table #
109 write(rbind(SEind1, SEind2), paste("SEind.txt", sep=""), ncolumns=2 )
110
111 # 2. Double click "matchzip.exe". A dos window will pop up. Type in SEind.txt. #
112 # This will produce many (n.edge) files at the current directory. #
113 # Then use the following code to prepare the edge plotting code. #
114 # "edgelines" should be dumped out and called in later when make edge plots. #
115
116 edgelines <- vector(mode="list", length=n.edge)
117
118 for(i in 1:n.edge){
119     edgelines[[i]] <- read.table(paste("output-", i, ".txt", sep=""), header=F,
120                                 na.strings="*")
121 }
122
123 edges <- edgelines
124 dput(edgelines, "edgelines.txt")
125
126 # 3. Double click "edgeneig.exe". A dos window will pop up. Type in SEind.txt #
127 # Two files will be produced (may take a while): #
128 # file 1 is the upper triangular of the W matrix for the edges; #
129 # file 2 is the number of 1s for each row of the upper triangular matrix. #
130
131 # 4. Produce the Wstar matrix which provides neighborhoods of the edges #
132
133 tempn <- scan(paste("file2.txt", sep=""))
134 tempneig <- scan(paste("file1.txt", sep=""))
135
136 Wstar <- matrix(0, nrow=n.edge, ncol=n.edge)
137 start <- 1
138 end <- 0
139
140 for(i in 1:n.edge){
141     if (tempn[i]>0){
142         start <- end+1
143         end <- start + tempn[i]-1
144         neig <- tempneig[start:end]
145         l <- tempn[i]
146         for (k in 1:l){
147             Wstar[i, neig[k]] <- Wstar[neig[k], i] <- -1
148         }
149     }
150 }

```

```

151
152 edge.adj <- mkAdj(Wstar)
153 dput(edge.adj, "edge.adj.txt")
154 edgeSum <- as.vector(rowSums(Wstar))
155 dput(edgeSum, "edgeSum.txt")
156 dput(Wstar, "Wstar.txt")
157
158 # 5. Remove files not needed any more #
159 for(i in 1:n.edge){
160     unlink(paste(i, ".txt", sep=""))
161     unlink(paste("output-", i, ".txt", sep=""))
162 }
163
164 unlink(paste("file1.txt", sep=""))
165 unlink(paste("file2.txt", sep=""))
166 unlink(paste("SEind.txt", sep=""))
167 #####
168
169
170 ###      chunk 3 - Areal wombling model      #####
171 # Three global covariates, spatial error
172 #  $\mu = \beta_0 + \beta_1 X_1 + \beta_2 X_2 + \beta_3 X_3 + \phi$ 
173
174 map <- readShapeSpatial("../hwa_wombling.shp")
175
176 temp <- map@data$WINTERTEMP
177 pop <- log(map@data$POP2000)
178 hemlock <- log(map@data$HEMLOCK)
179
180 Y <- (map$YEARINFEST-1951)*12
181 X1 <- pop
182 X2 <- hemlock
183 X3 <- temp
184
185
186 n.areas = length(Y)
187 adj <- dget("../edgefolder/Sadj.txt")
188 num = dget("../edgefolder/Snum.txt")
189 sumNumNeigh = sum(num)
190
191 # indexes required for plotting
192 ind1 <- ind2 <- rep(0, length(num))
193 ind1[1] <- 1
194 for(i in 1:length(num)){j <- i+1; ind1[j] <- num[i] + ind1[i]}
195 ind1 <- ind1[1:length(num)]
196 for(i in 1:length(num)){j <- i-1; ind2[i] <- ind1[i] + num[i]-1}
197
198 params <- 5 # number of parameters in the model
199
200 # initial values
201 phi1 <- rep(-10, n.areas)

```



```

202 phi2 <- rep(0,n.areas)
203 phi3 <- rep(10,n.areas)
204
205 inits.mod5 <- list(list(phi=phi1, sdy=15, sdphi=5, beta=rep(-5, params)),
206 list(phi=phi2, sdy=25, sdphi=5, beta=rep(0, params)), list(phi=phi3, sdy=35,
207 sdphi=5, beta=rep(10, params)))
208
209 dat.in.mod5 <- list("Y", "n.areas", "num", "sumNumNeigh", "adj", "X1", "X2",
210 "X3", "X4")
211
212 # call to Winbugs
213 mod <- bugs(data=dat.in.mod5, inits.mod5,
214 model.file="../../../areal_wombling.bug",
215 parameters.to.save=c("SLDRhat", "beta", "tau.err", "phi",
216 "tau.phi"), n.chains = length(inits.mod5), n.iter=200000,
217 n.burnin=100000, save.history=F, debug=TRUE,
218 bugs.directory="../../../WinBUGS14/", working.directory="...")
219
220 # read & summarize coda files
221 mod.coda <- read.coda.interactive()
222 # codaIndex.txt, coda1.txt, coda2.txt, coda3.txt
223 dimnames(mod.coda$coda1.txt)
224 samps <- mcmc.list(mcmc(mod.coda$coda1.txt[,c(323:328,651,652)]),
225 mcmc(mod.coda$coda2.txt[,c(323:328,651,652)]),
226 mcmc(mod.coda$coda3.txt[,c(323:328,651,652)]))
227 xyplot(samps)
228 gelman.plot(samps)
229 densityplot(samps)
230
231 merge.chains <- (mod.coda$coda1.txt + mod.coda$coda2.txt + mod.coda$coda3.txt)/3
232 SLDRhat <- merge.chains[,1:322]
233
234 rows <- nrow(SLDRhat)
235 cols <- ncol(SLDRhat)
236 phi <- merge.chains[,329:650]
237
238 # calculate posterior estimates of mu (sldrhat)
239 SLDRhat.samp <- matrix(0, ncol=cols, nrow=rows)
240 phi.samp <- matrix(0, ncol=cols, nrow=rows)
241 for(i in 1:n.areas){
242   from<-(i-1)*rows+1
243   to<-i*rows
244   SLDRhat.samp[,i]<- SLDRhat[from:to]
245   phi.samp[,i] <- phi[from:to]
246 }
247
248 #c alculate differences in spread dates across county edges
249 delta.sldr <- matrix(0, ncol=sum(num)/2,nrow=rows)
250 delta.phi <- matrix(0, ncol=sum(num)/2,nrow=rows)
251 k <- 0
252 for( i in 1:n.areas){

```

```

253     for(j in ind1[i]:ind2[i]){
254         if(adj[j]>i){
255             k<-k+1
256             delta.sldr[,k]<-abs(SLDRhat.samp[,i] - SLDRhat.samp[,adj[j]])
257             delta.phi[,k]<-abs(phi.samp[,i] - phi.samp[,adj[j]])}}
258
259 # Boundary likelihood values
260 p.sldr.5years <- apply(apply(delta.sldr,2,cut.func.5years)/rows,2,sum)
261 p.phi.5years <- apply(apply(delta.phi,2,cut.func.5years)/rows,2,sum)
262
263 # color palette for plotting boundaries
264 n.col = 4
265 col.br <- colorRampPalette(c("gray", "lightpink2", "red2", "red4"))
266 col.pal <- col.br(n.col)
267
268 # breaks for boundary groupings & legend text
269 br <- c(0.0,0.4,0.6,0.9,1.0)
270 leg.txt <- paste("(",br[n.col]," ~ ",br[n.col+1],")",sep="")
271 for(i in (n.col-1):1){
272     leg.txt <- append(leg.txt, paste("(", br[i], " ~ ", br[i+1], ")", sep=""),)
273 }
274 leg.txt <- rev(leg.txt)
275
276 # Plot maps with boundary probabilities
277 edgelines <- dget("../edgefolder/edgelines.txt")
278
279 # map of mu-based boundaries
280 probPlot(map, edgelines, p.sldr.5years, n.col, add=F, col.pal=col.pal)
281 legend(locator(), legend=leg.txt, col=col.pal, lty="solid", lwd=c(2,3,4,5),
282        cex=1.8, ncol=1,
283        bty="n", title="Boundary Probability")
284
285 # map of phi-based boundaries
286 probPlot(map, edgelines, p.phi.5years, n.col, add=F, col.pal=col.pal)
287 legend(locator(), legend=leg.txt, col=col.pal, lty="solid", lwd=c(2,3,4,5),
288        cex=1.8, ncol=1,
289        bty="n", title="Boundary Probability")
290 #####
291
292
293 ###      chunk 4 - Local edge wombling model      #####
294 # Three global covariates, spatial error
295 # model will not run using R2WinBUGS for some reason
296 # must copy and paste model, inits, data and run directly in winBUGS
297
298
299 map <- readShapeSpatial("../hwa_wombling.shp")
300 Y <- (map$YEARINFEST-1951)*12
301 mapDat <- map@data[,7:9]
302
303 # prepare data for edge wombling

```



```

355 dat.in.mod10 <- list(sumNumNeigh=sumNumNeigh, n.areas=n.areas, Y=Y, num=num,
356                      adj=adj, X1=X1, X2=X2, X3=X3)
357 edit(dat.in.mod10)
358
359
360 #call to Winbugs
361 mod10 <- bugs(data=dat.in.mod10, inits.mod10, model.file="...edge_womble.bug",
362 parameters.to.save=c("SLDRhat", "beta", "tau.err", "phi", "psi"),
363 n.chains = length(inits.mod10), n.iter=20000, n.burnin=10000,
364 save.history=F, debug=TRUE, bugs.directory=".../WinBUGS14/", codaPkg=T,
365 working.directory="...")
366
367 # read & summarize coda files
368 mod.coda <- read.coda.interactive()
369 # codaIndex.txt, coda1.txt, coda2.txt, coda3.txt
370 dimnames(mod.coda$coda1.txt)
371 samps <- mcmc.list(mcmc(mod.coda$coda1.txt[,c(794:798, 1592:1594)]),
372 mcmc(mod.coda$coda2.txt[,c(794:798, 1592:1594)]),
373 mcmc(mod.coda$coda3.txt[,c(794:798, 1592:1594)]))
374 xyplot(samps)
375 gelman.plot(samps)
376 densityplot(samps)
377
378 merge.chains <- (mod.coda$coda1.txt + mod.coda$coda2.txt + mod.coda$coda3.txt)/3
379 SLDRhat <- merge.chains[,1:793]
380 phi <- merge.chains[,799:1576]
381 psi <- merge.chains[,1577:1591]
382
383 rows <- nrow(SLDRhat)
384
385 # Boundary likelihood values at 5 years
386 p.sldr.5years <- apply(apply(abs(SLDRhat),2,cut.func.5years)/rows,2,sum)
387 p.phi.5years <- apply(apply(abs(phi),2,cut.func.5years)/rows,2,sum)
388 p.psi.5years <- apply(apply(abs(psi),2,cut.func.5years)/rows,2,sum)
389
390 num1 <- ifelse(num==0,0,1)
391
392 #combine island vector with index and sort
393 indx <- seq(1:length(Y))
394 srt <- as.data.frame(cbind(num1, indx))
395 srt <- srt[order(srt$num1, srt$indx),]
396
397 # bind phi and psi and then to srt df
398 phiX <- c(p.psi.5years, p.phi.5years)
399 srt <- cbind(srt,phiX)
400
401 # sort to original order and extract new psi vector
402 phi.df <- srt[order(srt$indx),]
403 p.phi.5years <- phi.df$phiX
404
405 # color palette for plotting boundaries

```

```

406 n.col = 4
407 col.br <- colorRampPalette(c("gray", "lightpink2", "red2", "red4"))
408 col.pal <- col.br(n.col)
409
410 # breaks for boundary groupings & legend text
411 br <- c(0.0,0.4,0.6,0.9,1.0)
412 leg.txt <- paste("(",br[n.col]," ~ ",br[n.col+1],")",sep="")
413 for(i in (n.col-1):1){
414     leg.txt <- append(leg.txt, paste("(", br[i], " ~ ", br[i+1], ")", sep=""),)
415 }
416 leg.txt <- rev(leg.txt)
417
418 # Plot maps with boundary probabilities
419 edgelines <- dget("../edgefolder/edgelines.txt")
420
421 # map of mu-based boundaries
422 probPlot(map, edgelines, p.sldr.5years, n.col, add=F, col.pal=col.pal)
423 legend(locator(), legend=leg.txt, col=col.pal, lty="solid", lwd=c(2,3,4,5),
424        cex=1.8, ncol=1, bty="n", title="Boundary Probability")
425
426 # map of phi-based boundaries
427 probPlot(map, edgelines, p.phi.5years, n.col, add=F, col.pal=col.pal)
428 legend(locator(), legend=leg.txt, col=col.pal, lty="solid", lwd=c(2,3,4,5),
429        cex=1.8, ncol=1, bty="n", title="Boundary Probability")
430
431 # Boundary likelihood values at 3 years
432 p.sldr.3years <- apply(apply(abs(SLDRhat),2,cut.func.3years)/rows,2,sum)
433 p.phi.3years <- apply(apply(abs(phi),2,cut.func.3years)/rows,2,sum)
434 p.psi.3years <- apply(apply(abs(psi),2,cut.func.3years)/rows,2,sum)
435
436 num1 <- ifelse(num==0,0,1)
437
438 # combine island vector with index and sort
439 indx <- seq(1:length(Y))
440 srt <- as.data.frame(cbind(num1, indx))
441 srt <- srt[order(srt$num1, srt$indx),]
442
443 # bind phi and psi and then to srt df
444 phiX <- c(p.psi.3years, p.phi.3years)
445 srt <- cbind(srt,phiX)
446
447 # sort to original order and extract new psi vector
448 phi.df <- srt[order(srt$indx),]
449 p.phi.3years <- phi.df$phiX
450
451 # map of mu-based boundaries
452 probPlot(map, edgelines, p.sldr.3years, n.col, add=F, col.pal=col.pal)
453 legend(locator(), legend=leg.txt, col=col.pal, lty="solid", lwd=c(2,3,4,5),
454        cex=1.8, ncol=1, bty="n", title="Boundary Probability")
455
456 # map of phi-based boundaries

```

```

457 probPlot(map, edgelines, p.phi.3years, n.col, add=F, col.pal=col.pal)
458 legend(locator(), legend=leg.txt, col=col.pal, lty="solid", lwd=c(2,3,4,5),
459       cex=1.8, ncol=1, bty="n", title="Boundary Probability")
460 #####
461
462
463 # functions needed to format data & results and make plots
464
465 probPlot <- function(map, edgelines, y, n.col, add, col.pal){
466   require(classInt)
467   polylist <- map@polygons
468   br <- c(0, 0.4, 0.6, 0.9, 1)
469   y.grp <- findInterval(y, vec=br, rightmost.closed = TRUE, all.inside = TRUE)
470   y.shad <- col.pal[y.grp]
471   linewidth <- y.grp + 1
472
473   plot(map, axes=F, auxvar=Y, add=add)
474
475   for (i in 1:length(edgelines)){
476     lines(as.matrix(edgelines[[i]]),col=y.shad[i],lwd=linewidth[i])
477   }
478 }
479
480
481 #functions to calculate boundary probs at different thresholds
482 cut.func.1years <- function(x){
483   c.ind<-as.numeric(x>12)
484   return(c.ind)}
485
486 cut.func.2years <- function(x){
487   c.ind<-as.numeric(x>24)
488   return(c.ind)}
489
490 cut.func.3years <- function(x){
491   c.ind<-as.numeric(x>36)
492   return(c.ind)}
493
494 cut.func.4years <- function(x){
495   c.ind<-as.numeric(x>48)
496   return(c.ind)}
497
498 cut.func.5years <- function(x){
499   c.ind<-as.numeric(x>60)
500   return(c.ind)}
501
502 cut.func.6years <- function(x){
503   c.ind<-as.numeric(x>72)
504   return(c.ind)}
505
506 cut.func.8years <- function(x){
507   c.ind<-as.numeric(x>96)

```

```
508     return(c.ind)}
509
510 cut.func.10years <- function(x){
511     c.ind<-as.numeric(x>120)
512     return(c.ind)}
513
514 # functions need to calculate deltas across boundries
515 delta.calculate <- function(x, ind1, ind2, n){
516     delta<-rep(0,n)
517     for (k in 1:n){
518         i <- ind1[k]
519         j <- ind2[k]
520         delta[k] <- x[j] - x[i]
521     }
522     return(delta)
523 }
524
525 weight.calculate <- function(x, ind1, ind2, n){
526     delta<-rep(0,n)
527     for (k in 1:n){
528         i <- ind1[k]
529         j <- ind2[k]
530         delta[k] <- x[j] - x[i]
531     }
532     return(delta)
533 }
```